Computer-aided design-based circuit model of microstrip line for terahertz interconnects technology

Yogendra K. Awasthi[1], Himanshu Singh[1], Manish Sharma[2], Sarita Kumari[3], Anand K. Verma[4]

[1]*Antenna Fabrication & Measurement Laboratory, Electronics & Communication Engineering, Manav Rachna University, Faridabad, Haryana 121 001, India*
[2]*Department of Electronics & Communication Engineering, SGT University, Gurugram, Haryana 122505, India*
[3]*Department of Physics, University of Rajasthan, Jaipur 302 004, Rajasthan, India*
[4]*Microwave Research Laboratory, Department of Electronic Science, South Campus, University of Delhi, New Delhi 110 021, India*
E-mail: yogendra@mru.edu.in

Published in *The Journal of Engineering*; Received on 10th March 2017; Accepted on 3rd August 2017

Abstract: In this study, presented a computer-aided design-based circuit model which is applicable to microstrip transmission line for terahertz interconnects technology in circuit simulator. Comparison of modified Kirschning and Jansen for dispersion and modified characteristic impedance for characteristic impedance models with full-wave electromagnetic (EM) simulator are investigated which shows $<1\%$ deviation for w/h range $0.1 \leq w/h \leq 100$, conductor thickness $0.001 \leq t/h \leq 0.2$, wavelength range $8.7\ \mu\text{m} \leq \lambda g \leq 8.7$ m and substrate permittivity $1.0 \leq \varepsilon_r \leq 200$. Modified conductor loss for conductor loss and modified dielectric loss (MDL) for dielectric loss are also investigated and compared with EM simulator, which shows deviation of <1 dB for above said electrical and physical sets of range of parameters. Calculation of line parameters: (f, t), (f, α), $R(f)$, $L(f)$, $C(f)$, $G(f)$ by using the effect of dispersion, characteristic impedance and losses which shows $<1\%$ deviation with experimental data available. Accuracy of the circuit model are also verified for interconnects made by aluminium ($\sigma_o = 3.7 \times 10^7$ S/m), tungsten ($\sigma_o = 1.0 \times 10^7$ S/m) and tungsten–silicide ($\sigma_o = 3.3 \times 10^6$ S/m) conductors which used in very large scale integration/ultra large scale integration (VLSI/ULSI) technology.

1 Introduction

Microwave integrated circuit (MIC) and monolithic MIC (MMIC) are important for *analog* high-frequency technology. These are also important as the high-speed *interconnects* for digital applications. The microstrip line is important for such applications. The microstrip line has found its applications from 0.01 GHz to 10 THz frequency range. The objective of the terahertz (THz) electronics programme is to develop the critical device and integration technologies necessary to realise compact, high-performance electronic circuits that operate at centre frequencies exceeding 1.0 THz.

The objective of the THz electronics programme is to develop the critical device and integration technologies necessary to realise compact, high-performance electronic circuits that operate at centre frequencies exceeding 1.0 THz. The THz interconnect opens high potential new revenue to solve long standing interconnects issues [1–9]. Plastic sheet and ceramic thin plates are normally used as substrates for the hybrid MIC technology. The planar lines are also used on the semiconducting substrates such as silicon (Si) and gallium arsenide along with built-in active devices on the same substrates. Microstrip line is a lossy and dispersive planar line [10]. Several closed-form models have been developed to determine frequency-dependent effective relative permittivity and the characteristic impedance of a microstrip line [11]. Similarly, closed-form model is reported to compute the dielectric and conductor losses of a microstrip line for the analysis and synthesis. The full-wave methods such as method of moments, spectral domain analysis (SDA), finite difference time-domain (TD) method, and finite element method (FEM) have been developed for two-dimensional (2D) and 3D structures. On the basis of these methods, several commercial electromagnetic (EM) simulators such as Sonnet, high-frequency structure simulator (HFSS), CST Microwave Studio etc. [12] have been developed. The microstrip line parameters: effective relative permittivity, characteristic impedance, dielectric loss and conductor loss can be determined using these simulators.

The available microstrip dispersion models [13] have not been tested for the THz frequency range. These models also did not include the effect of conductor thickness of the dynamic effective relative permittivity, except the logistic dispersion model (LDM) to some extent [14]. Thus, the existing dispersion model must be improved to include the effect of the conductor thickness, so that model could operate up to THz range in realistic manner. It has been also reported that carbon nano-tubes for new millimetre (mm) to THz interconnects for nano-packaging applications [15].

In this paper, improved models for dispersion and losses have proposed up to 10 THz. Several variations in the models have tested against the results obtained from EM full-wave simulator. We have noted that different variations in the main models work in better way in different parametric ranges and determines the parametric ranges of the *individual models*, i.e. the *direct model* and suggested the *integrated closed-form model* for the microstrip line that computes accurately its line parameters from 0.01 GHz to 10 THz. Next, the *integrated closed-form model* is used to get frequency-dependent primary line parameters – $R(f)$, $L(f)$, $C(f)$ and $G(f)$, i.e. line resistance, inductance, capacitance and conductance per unit length (p.u.l.), respectively. These line parameters are needed to design of the microwave circuits and interconnect. The primary line parameters are finally used to develop circuit model of the microstrip line. It helps to compute the dynamic dispersion and total losses of a practical microstrip line. It takes care of the effect of losses on the effective relative permittivity and effect of the relative permittivity of the substrate on the losses. These individual models, integrated closed-form models and circuit models are also useful to analyse low/high-speed pulses during propagation of pulses over interconnects.

1.1 Microstrip dispersion models

Over the years more than ten closed-form expressions have been developed to compute the frequency-dependent effective relative

doi: 10.1049/joe.2017.0078

permittivity of the open microstrip line [16]. The dispersion in microstrip shows the presence of *inflection frequency*, i.e. a frequency at which the slope of frequency-dependent effective relative permittivity changes its nature. The dispersion must meet Schneider's physical conditions and also meet Sadiku and Musa conditions [17]. The models have varying order of error over different parametric ranges. It has been compared accuracy of these models over set of experimental data and has also been compared against the SDA [18, 19] but all models developed for the zero strip conductor thickness, means without conductor loss; therefore, not suitable for practical interconnects design.

2 Proposed dispersion model analysis

2.1 Modified Kirschning and Jansen (MKJ)-model

The microstrip line, with finite conductor thickness is shown in Fig. 1. Hammerstad and Jensen [20] have suggested the following highly accurate model to compute the static effective relative permittivity:

$$\varepsilon_{r\,\mathrm{eff}}(w/h,\ \varepsilon_r) = 1 + q(\varepsilon_r - 1) \tag{1}$$

where ε_r is relative permittivity of the substrate. The filling-factor q of the microstrip line is given below:

$$q = \frac{F+1}{2}, \quad F = \left(1 + 10\frac{h}{w}\right)^{-a\times b} \tag{2}$$

where

$$a = 1 + \frac{1}{49}\ln\left(\frac{\left((w/h)\right)^4 + \left((w/52h)\right)^2}{\left((w/h)\right)^4 + 0432}\right) + \frac{1}{18.7}\ln\left(1 + \left(\frac{w}{h18.1}\right)^3\right),$$

$$b = 0.564 \cdot \left(\frac{\varepsilon_r - 0.9}{\varepsilon_r - 3}\right)^{0.053}$$

Also, ***h*** is the height of substrate and ***w*** is the width of microstrip.

The static effective relative permittivity $\varepsilon_{r\,\mathrm{eff}}(w/h,\ \varepsilon_r)$ is also obtained from the variational method. Bahl and Garg have suggested the following empirical expression to account for the effect of the finite thickness (t) on the effective relative permittivity which was valid for both the *thin microstrip* ($0.0 \le t/h \le 0.05$) and *thick microstrip* ($0.05 \le t/h \le 0.2$) line [21]:

$$\varepsilon_{r\,\mathrm{eff}}(w/h,\ \varepsilon_r,\ t) = \varepsilon_{r\,\mathrm{eff}}(w/h,\ \varepsilon_r) - \frac{(\varepsilon_r - 1)\cdot(t/h)}{4.6\sqrt{(w/h)}} \tag{3}$$

Typically, the strip thickness is 0.45–3.0 μm in MMICs and 3.0–90 μm in hybrid MICs used [22].

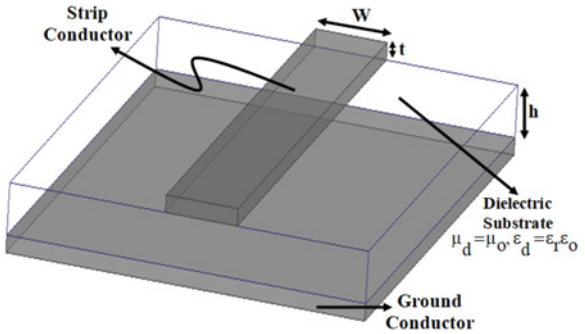

Fig. 1 *Microstrip line structure with finite strip conductor thickness*

The width of the strip conductor is also enlarged due to the finite strip conductor. The effective width is given by the following expression [23].

The KJ model is modified to take into account the finite thickness of strip conductor. This is achieved by replacing the physical strip width w with effective strip width $w_{\mathrm{eff}}(w/h,\ t)$ given by (4)

$$w_{\mathrm{eff}}(w/h,\ t) = w + \Delta w \quad (a),$$

$$\Delta w = \begin{cases} \dfrac{t}{\pi}\cdot\left(1 + \ln\dfrac{4\cdot\pi\cdot w}{t}\right) & \text{for } \dfrac{w}{h} \le \dfrac{1}{2\pi} \\ \dfrac{t}{\pi}\cdot\left(1 + \ln\dfrac{2\cdot h}{t}\right) & \text{for } \dfrac{w}{h} > \dfrac{1}{2\pi} \end{cases} \quad (b) \tag{4}$$

The MKJ-dispersion model is given below:

$$\varepsilon_{r\,\mathrm{eff}}(w_{\mathrm{eff}},\ h_{\mathrm{cm}},\ t,\ \varepsilon_r,\ f) = \varepsilon_r - \frac{\varepsilon_r - \varepsilon_{r\,\mathrm{eff}}(w_{\mathrm{eff}}/h,\ \varepsilon_r,\ t)}{1 + P(f_{\mathrm{GHz}})} \tag{5}$$

In the above expression, frequency (f) and substrate thickness (h) are in gigahertz and centimetres, respectively. The KJ model is valid for $0.1 \le w/h \le 100$, $1 < \varepsilon_r \le 20$ and $0 < f \times h \le 3.9$ GHz cm with deviation within 0.6% from the results of SDA. However, from other full-wave sources deviation is about 1%. Almost same accuracy is maintained even by incorporating the conductor thickness in the MKJ model. The results are discussed in the next section. Therefore, the LDM is also summarised below:

$$P(f_{\mathrm{GHz}}) = P_1\cdot P_2\cdot\left\{(0.1844 + P_3P_4)\cdot 10\cdot f_{\mathrm{GHz}}\cdot h\right\}^{1.5763}$$

$$P_1 = 0.27488 + \frac{w_{\mathrm{GHz}}}{h}\left(\begin{matrix}0.6315 + \left(\dfrac{0.525}{(1 + 0.157\cdot f_{\mathrm{GHz}}\cdot h)^{20}}\right) \\ -0.065683\exp\left(\dfrac{-8.7513\cdot w_{\mathrm{eff}}}{h}\right)\end{matrix}\right),$$

$$P_2 = 0.33622\cdot(1 - \exp(-0.03442\cdot\varepsilon_r))$$

$$P_3 = 0.0363\exp(-4.6\cdot w_{\mathrm{eff}}/h)\cdot\left(1 - \exp\left(\frac{-f_{\mathrm{GHz}}\cdot h}{3.87}\right)^{4.97}\right),$$

$$P_4 = 1 + 2.751\cdot(1 - \exp(-\varepsilon_r/15.916)^8) \tag{6}$$

2.2 Logistic DM

The LDM is based on the phenomenological microstrip dispersion law. It is expressed through the first-order differential equation which is given below:

$$\varepsilon_{r\,\mathrm{eff}}(f) = \frac{\varepsilon_r}{1 + Me^{-K(f/f_i)}} - E\Delta\varepsilon_r(f) \quad (a)$$

$$\text{for} \quad 1 \le \varepsilon_r \le 20{:}E = \begin{cases} 0 & 0.1 \le w/h < 5 \\ 1 & w/h \ge 5 \end{cases} \quad (b), \tag{7}$$

$$\text{for} \quad 20 < \varepsilon_r \le 200{:}E = \begin{cases} 1 & 0.5 \le w/h < 1 \\ 0 & w/h \ge 1 \end{cases} \quad (c)$$

The parameters M and K are given by

$$M = \frac{\varepsilon_r - \varepsilon_{r\,\mathrm{eff}}(w/h,\ \varepsilon_r,\ t)}{\varepsilon_{r\,\mathrm{eff}}(w/h,\ \varepsilon_r,\ t)}\ (a),$$

$$K = \ln\left[\frac{3\cdot\varepsilon_{r\,\mathrm{eff}}(w/h,\ \varepsilon_r,\ t) - \varepsilon_r}{\varepsilon_{r\,\mathrm{eff}}(w/h,\ \varepsilon_r,\ t)}\right](b) \tag{8}$$

The inflection frequency is determined from the coupling frequency f_k, transverse magnetic (TM)

$$f_i = \frac{f_{k\,\mathrm{TM}}}{\sqrt{3}\left(1 + B(\Delta w/h)\right)^A} \ (a), \quad f_{k\,\mathrm{TM}} = c\frac{\tan^{-1}\left[\varepsilon_r\sqrt{(\varepsilon_{r\,\mathrm{eff}}(w/h,\ \varepsilon_r,\ t) - 1/\varepsilon_r - \varepsilon_{r\,\mathrm{eff}}(w/h,\ \varepsilon_r,\ t))}\right]}{2\pi h\sqrt{\varepsilon_r - \varepsilon_{r\,\mathrm{eff}}(w/h,\ \varepsilon_r,\ t)}} \ (b) \tag{9}$$

The parameters A and B are ε_r and w/h dependent. Finally, the relative permittivity deviation $\Delta\varepsilon_r(f)$ appearing in equation below showing correction in the model is given by:

$$\Delta\varepsilon_{r\,\mathrm{eff}}(f) = \frac{\mathrm{MK}\left(\varepsilon_r - \varepsilon_{r\,\mathrm{eff}}(0)\right)^{((k/f/f_i))}}{\left(1 + M\mathrm{e}^{-K((f/f_i))}\right)^2}\left(\frac{f}{f_i}\right) \quad f \le f_i \ (a) \quad \Delta\varepsilon_{r\,\mathrm{eff}}(f) = \frac{\mathrm{MK}\left(\varepsilon_r - \varepsilon_{r\,\mathrm{eff}}(0)\right)^{((k/f/f_i))}}{\left(1 + M\mathrm{e}^{-K((f/f_i))}\right)^2}\left(\frac{f_i}{f}\right) \quad f > f_i \ (b) \tag{10}$$

The LDM has also used the dispersive effective width. Both the improved models are compared against the results obtained from full-wave EM simulator which provides result for the quasi-transverse electromagnetic (TEM) mode only. Thus, they provide reliable results up to appearance of the first transverse electric (TE) mode and the models should be used only for $f < f_{\mathrm{TE}}$, where f_{TE} is given by

$$f_{\mathrm{TE}} = c/4 \cdot h \cdot \sqrt{\varepsilon_r - 1} \quad c = 3 \times 10^8\ \mathrm{m/s} \tag{11}$$

2.3 Comparison of results of proposed MKJ and LDM against EM simulator

The microstrip dispersion models assume that relative permittivity of the substrate is frequency dependent, is not true. A practical substrate is always lossy. Its real and imaginary parts are frequency dependent and related through Krammer–Kronig relation. The ionic and dipolar polarisations play the dominant role in determination of frequency-dependent complex relative permittivity of material commonly used in microwave applications. These polarisation types follows Debye's relaxation polarisation model. Debye's model follows Krammer–Kronig relation [24]. Thus, the microstrip dispersion and dielectric loss should account for the material dispersion according to Debye's model. However, the individual, i.e. the direct dispersion models presented above do not follow Debye's model. Such models are still useful for microwave analogue circuit applications. However, in time DA they give unrealisable response that does not follow the causality requirement.

Debye's models have been developed for substrate materials based on limited measurement of frequency-dependent relative permittivity and loss tangent. EM simulator incorporates these requirements on relative permittivity and loss tangent by *Debye's model* and also by *piecewise linear material model.* We have selected the second model for data generation to compare the MKJ model and LDM. Figs. 2*a–c* compares.

MKJ-dispersion model and LDM against the results obtained from EM simulator for the microstrip of w/h ratio 0.1, 1.0 and 10.0, respectively, and strip conductor thickness $t/h = 0.001$, 0.05, 0.1, 0.2. The average and maximum deviations in models, for w/h ratios 0.1, 1.0 and 10.0 are shown in Table 1. Thus, both models are equally acceptable from average deviation point of view.

However, careful analysis of results shows some important differences in the performance of both dispersion models. Figs. 2*a–c* show that with increase in the thickness of strip conductor, deviation on LDM increases from the results of EM simulator. As a matter of fact, for $w/h = 0.1$ and $t/h \ge 0.1$ LDM fails to work properly. For $w/h \ge 1$ LDM behaves properly; still in transition region 10–200 GHz, deviation in LDM is more as compared with that of the MKJ-dispersion model. Thus, we have to select MKJ model in the range of its better performance in order to develop the dispersion part of the *integrated closed-form model.*

Finally, we also noted that both the models are *partially casual* models for the TD point of view. Any arbitrary frequency-domain function cannot have a TD interpretation within the framework of causality that is important for digital signal processing. It is important for the TD characteristics for pulse propagation on microstrip line.

3 Proposed dielectric loss model analysis

Computation of both dielectric and conductor losses are important for narrowband analogue microwave circuits and for multi-gigabit wide-band signals on printed circuit board and also on chip configuration. The loss not only introduces attenuation of the signals but, far more important, distortion in digital pulses. The distortion will in turn introduce inter-symbol interference, which seriously limits the data rate or calls for equalisation. Therefore, it becomes very important to accurately characterise the TD behaviour of transmission lines on personal computer boards. However, existing model to compute the dielectric loss is non-causal that fails to correctly describe the TD effects. We have discussed previously that the dielectric loss is due to the imaginary part of the complex relative permittivity of the substrate material. However, in this section we report modified version of the classical dielectric loss expression to include frequency-dependent tan $\delta(f)$ for high-frequency range, so that classical model works up to THz. Accuracy of the MDL is tested again the results of EM simulator that uses *piecewise linear material model.* Thus, our suggested model could be a partially causal model.

3.1 MDL model

The dielectric loss is caused by an imperfect lossy substrate material which described by the complex relative permittivity. On the other hand, it is also calculated by the loss tangent tan $\delta(f = 0)$ or by the static conductivity σ_0 of a substrate. These parameters are related through following expressions:

$$\varepsilon_r^* = \varepsilon_r' - \mathrm{j}\varepsilon_r'' \Rightarrow \varepsilon_r^* = \varepsilon_r - \mathrm{j}\varepsilon_r \tan\,\delta(f = 0) \quad (a)$$
$$\text{where } \mathrm{Re}(\varepsilon_r^*) = \varepsilon_r' = \varepsilon_r, \quad \mathrm{Im}(\varepsilon_r^*) = \varepsilon_r'' = \varepsilon_r \tan\,\delta(f = 0) \quad (b)$$
$$\tan\,\delta(f = 0) = \frac{\varepsilon_r''}{\varepsilon_r'} = \frac{\sigma_0}{\omega\varepsilon_0\varepsilon_r} \quad \varepsilon_r'' = \frac{\sigma_0}{\omega\varepsilon_0} \quad (c)$$
$$\tan\,\delta(f = 0) = \frac{\sigma_f/\omega + \varepsilon_r''}{\varepsilon_r'} \quad (d) \tag{12}$$

In (12c) for the loss tangent, contribution of conductivity σ_f has been ignored due to free charges and also considered only ε_r'', that is, polarisation loss. The correct expression is (12d). The dielectric loss of a microstrip is computed by the following classical formula:

$$\alpha_d = \frac{\pi[\varepsilon_{r\,\mathrm{eff}}(0) - 1]}{\lambda_0[\varepsilon_r - 1]}\frac{\varepsilon_r \tan\,\delta}{\sqrt{\varepsilon_{r\,\mathrm{eff}}(0)}} \quad \mathrm{Np/length} \tag{13}$$

In the above expression, static effective relative permittivity is independent of frequency and computed using Hammerstad and Jensen formula summarised by (1). The loss tangent tan δ is also frequency independent and material dispersion is also ignored, as needed by Debye's model. However, this model has been in use for microwave and mm-wave applications over narrowband.

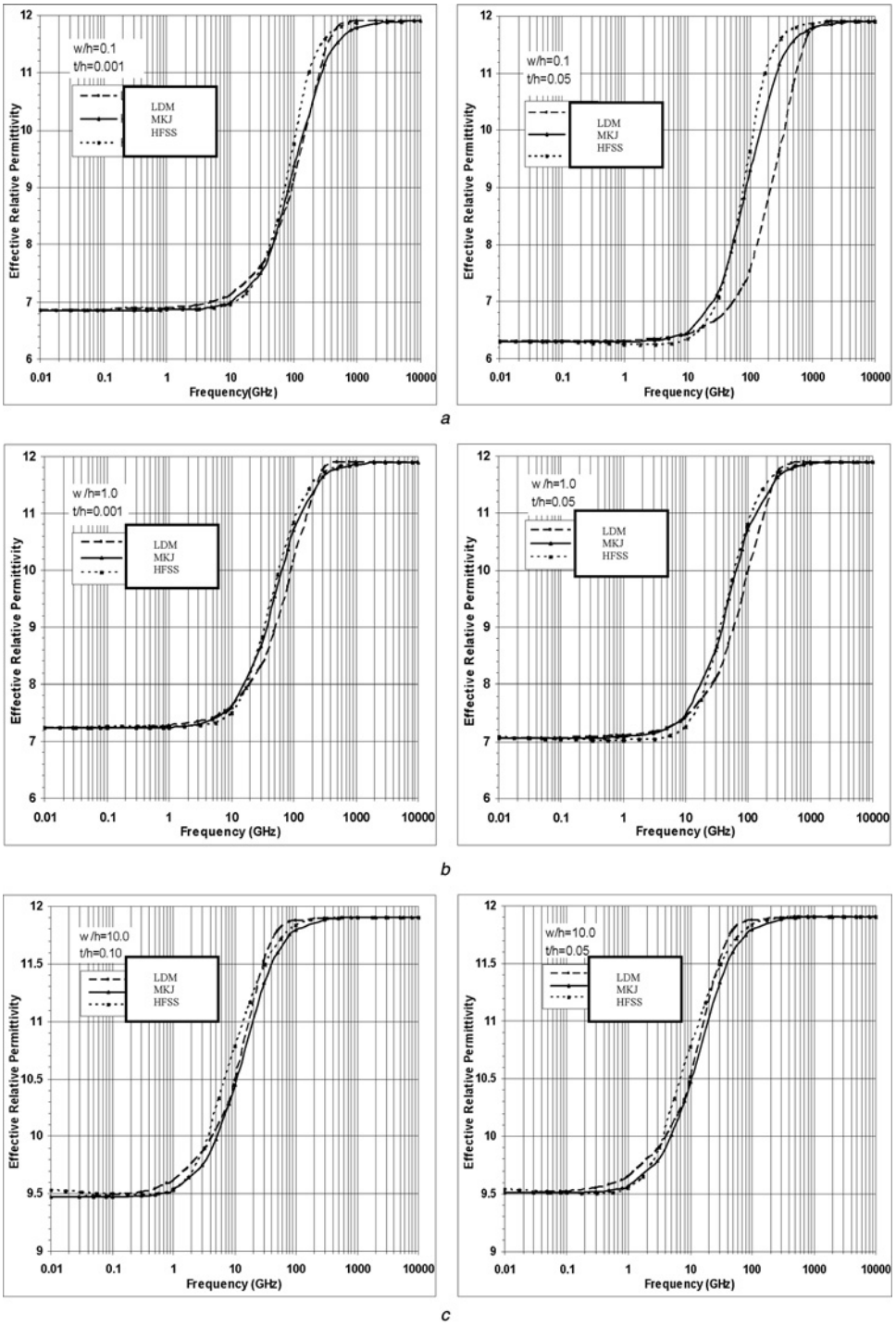

Fig. 2 *Effective relative permittivity for*
a $w/h = 0.1$, $h = 0.45$ mm, $\varepsilon_r = 11.9$, $t/h = 0.001, 0.05$
b $w/h = 1.0$, $h = 0.45$ mm, $\varepsilon_r = 11.9$, $t/h = 0.001, 0.05$
c $w/h = 10.0$, $h = 0.45$ mm, $\varepsilon_r = 11.9$, $t/h = 0.001, 0.05$

We can easily accommodate effect of the finite conductor thickness and dispersion in computation of dynamic effective relative permittivity as discussed in the previous section. For computing the dielectric loss above 100 GHz, we can empirically modify the loss tangent on making conductivity of the substrate frequency dependent. Increase in conductivity of the strip conductor is suggested empirically [25, 26].

The range of applicability is determined by comparing the results on dielectric loss against the results of full-wave EM simulator. The suggested expression for the frequency-dependent loss tangent is

$$\sigma(f) = \frac{\sigma_0}{\sqrt{1 + C_0 f_{\text{GHz}}}} \quad (a),$$

$$\tan\,\delta(f) = \frac{\sigma(f)}{\omega\varepsilon_0\varepsilon_r} = \frac{1}{\omega\varepsilon_0\varepsilon_r}\frac{\sigma_0}{\sqrt{1 + C_0 f_{\text{GHz}}}} \quad \text{where } C_0 = 0.045 \quad (b) \tag{14}$$

doi: 10.1049/joe.2017.0078

Table 1 Percentage deviation of MKJ model and LDM against EM simulator for effective relative permittivity from 10 MHz to 10 THz

t/h	Effective relative permittivity											
	$w/h = 0.1$, $h = 0.45$ mm, $\varepsilon_r = 11.9$				$w/h = 1.0$, $h = 0.45$ mm, $\varepsilon_r = 11.9$				$w/h = 10.0$, $h = 0.45$ mm, $\varepsilon_r = 11.9$			
	MKJ model		LDM		MKJ model		LDM		MKJ model		LDM	
	%Average deviation	%Maximum deviation	%Average deviation	%Maximum. deviation	%Average deviation	%Maximum deviation	%Average deviation	%Maximum deviation	%Average deviation	%Maximum. deviation	%Average deviation	%Maximum deviation
0.0	0.48	2.5	1.30	5.0	1.30	5.5	1.14	5.5	0.40	1.50	0.71	3.50
0.001	0.36	2.6	1.43	4.4	0.91	4.3	1.24	6.2	0.43	2.50	0.45	2.40
0.05	0.38	2.2	3.5	7.5	0.40	5.2	1.45	4.5	0.45	1.50	0.71	3.50
0.10	0.31	2.4	LDM fails		0.39	5.4	1.63	6.7	0.40	2.70	0.45	2.90
0.15	0.29	2.2			0.57	3.5	1.55	5.9	0.43	2.75	0.35	2.30
0.20	0.34	2.1			0.67	3.9	1.67	5.7	0.49	2.77	0.35	2.35

The constant C_0 could be improved empirically for different substrates in different frequency ranges. The modified expression to compute dielectric loss of a microstrip up to THz is given below:

$$\alpha_d(f) = \frac{\varepsilon_r}{\sqrt{\varepsilon_{r\,\mathrm{eff}}(w_{\mathrm{eff}},\ h,\ t,\ \varepsilon_r,\ f)}} \cdot \frac{\varepsilon_{r\,\mathrm{eff}}(w_{\mathrm{eff}},\ h,\ t,\ \varepsilon_r,\ f) - 1}{\varepsilon_r - 1} \frac{\pi}{\lambda_0} \tan\ \delta(f) \quad \mathrm{Np/m} \tag{15}$$

3.2 *Comparison of results of the proposed MDL against EM simulator*

Computation of dielectric loss using (15) depends on effective relative permittivity and loss tangent. Both these parameters could be either static or frequency dependent that is dynamic. The effective relative permittivity is also dependent on the strip conductor thickness. Thus, we can form four models out of these two parameters – Model# 1–{($\varepsilon_{\mathrm{reff}}(f)$, tan $\delta(0)$}, using dynamic effective relative permittivity and static loss tangent; Model# 2–{($\varepsilon_{\mathrm{reff}}(0)$, tan $\delta(0)$}, static effective relative permittivity and static loss tangent; Model# 3–{($\varepsilon_{\mathrm{reff}}(f)$, tan $\delta(f)$}, dynamic effective relative permittivity and frequency-dependent loss tangent; Model# 4–{($\varepsilon_{\mathrm{reff}}(0)$, tan $\delta(f)$}, static effective relative permittivity frequency-dependent loss tangent. Fig. 3 compares the dielectric loss in Np/m computed by these models against the results obtained from EM simulator for *w/h* 0.1, 1.0 and 10.0, respectively. The strip and ground conductors are perfect conductors during this analysis

(see equation (16) at the bottom of the next page)

We further note that the deviation in computed loss is nearly independent of *w/h*. The percentage deviation in frequency range 100 GHz—1.0 THz could be improved by properly selecting the empirical constant C_0 in (14). EM simulator uses causal dielectric model, whereas proposed models are partially causal. However, the nature of dielectric loss computed by a combination of model# 2 and model# 4 follows nature of the dielectric loss obtained from the EM simulator and also deviation is not very high, it is in the range of deviation obtained from various full-wave methods [27]. In summary, (15) should be used in two ranges in the form of model# 2 and model# 4.

Equation (15) with ranges defined in (16) forms a part of the integrated *closed-form model* to compute line parameters of a loss and dispersive microstrip line.

4 Proposed conductor loss model analysis

Several full-wave methods have been developed to compute the conductor loss of a microstrip line. These methods have been adapted to several commercial EM simulators such as HFSS, Sonnet and CST Microwave Studio etc. [11]. The closed-form models based on Wheeler's incremental rule and perturbation method have been developed. It uses Wheeler's incremental rule to compute conductor loss of microstrip that is valid for $t/\delta_s \geq 7$. Moreover, they have used expression for the real and static characteristic impedances that give us non-causal response in TD [28]. The validity range has been also improved to $t/\delta_s \geq 1.1$ leaving model non-casual. The perturbation method is applicable for $t < \delta_s$ also and it uses real characteristic impedance only. Thus, this method is also non-causal. None of these models are applicable at low frequency at which current is uniformly distributed inside the conducting strip. We examine the validity range of both models to compute the conductor loss from 0.01 GHz to 10 THz. We have also considered frequency-dependent conductivity as part of both models and attempted to examine range of their applicability by comparing the computed results using the models against the

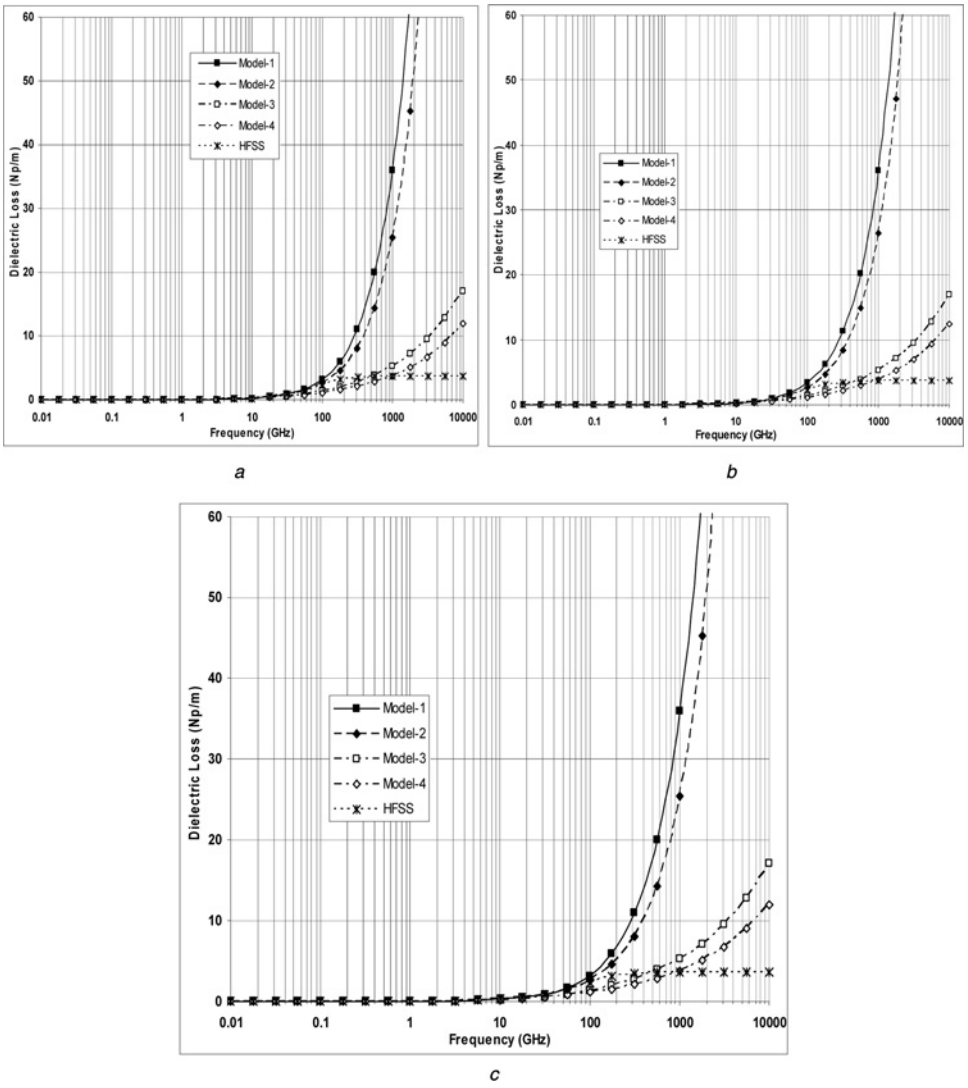

Fig. 3 *Dielectric loss for h = 0.45 mm, $\varepsilon_r = 11.9$, tan δ (0) = 0.001*
a w/h = 0.1
b w/h = 1.0
c w/h = 10.0

results from EM simulator. As the characteristic impedance is needed in this computation, therefore, we also summarise expressions for its computation.

4.1 Characteristic impedance

A closed-form approximate expression for the quasi-static characteristic impedance of a microstrip line developed by Hammerstad and Jensen [23] has been adopted and given below:

$$Z_0(w_{\text{eff}},\ h,\ \varepsilon_{\text{r}}=1)=\frac{377}{2\pi}\cdot\ln\left(F_1\frac{h}{w_{\text{eff}}}+\sqrt{1+\left(\frac{2h}{w_{\text{eff}}}\right)^2}\right)\quad(a)$$

$$\text{where } F_1=6.0+(2\pi-6)\cdot\exp\left(-\left(30.666\cdot\frac{h}{w_{\text{eff}}}\right)^{0.7528}\right)\quad(b)\tag{17}$$

$$\text{range for model\#2:}\{(\varepsilon_{\text{reff}}(0),\ \tan\delta(0)\}:\frac{30\times10^2}{\sqrt{\varepsilon_{\text{r}}}}<\lambda_g<\frac{30\times10^{-2}}{\sqrt{\varepsilon_{\text{r}}}}\text{cm}\quad(a)$$

$$\text{range for model\#4: }\{(\varepsilon_{\text{reff}}(0),\ \tan\delta(f)\}:\frac{30\times10^{-2}}{\sqrt{\varepsilon_{\text{r}}}}<\lambda_g<\frac{30\times10^{-3}}{\sqrt{\varepsilon_{\text{r}}}}\text{cm}\quad(b)$$

$$\text{range above 1.0 THz i.e for:}\frac{30\times10^{-3}}{\sqrt{\varepsilon_{\text{r}}}}<\lambda_g<\frac{30\times10^{-4}}{\sqrt{\varepsilon_{\text{r}}}}\text{cm}\quad(c)\tag{16}$$

$$\text{use results computed at }\lambda_g=\frac{30\times10^{-3}}{\sqrt{\varepsilon_{\text{r}}}}\text{rcm}\cdot\text{ where }\quad\lambda_g=\frac{\lambda_0}{\sqrt{\varepsilon_{\text{r}}}}\quad(d)$$

doi: 10.1049/joe.2017.0078

In (17), w_{eff} accounts for the effect of conductor thickness on characteristic impedance of a microstrip line. The frequency-dependent characteristic impedance of a microstrip line with finite strip thickness is computed as follows:

$$Z_{\text{L}}(w_{\text{eff}},\ h,\ t,\ \varepsilon_{\text{r}}, f) = \frac{Z_0(w_{\text{eff}},\ h,\ \varepsilon_{\text{r}} = 1)}{\sqrt{\varepsilon_{\text{r eff}}(w_{\text{eff}},\ h,\ t,\ \varepsilon_{\text{r}}, f)}} \tag{18}$$

The conductor thickness-dependent effective relative permittivity $\varepsilon_{\text{r eff}}(w_{\text{eff}},\ h,\ t,\ \varepsilon_{\text{r}}, f)$ is obtained from the MKJ model discussed in Section 2.1. As we know, impedance can be calculated by three conventional methods as power-current, power-voltage and voltage-current. Equation (18) has been based on power-current method.

4.2 Modified conductor loss (MCL) model

The conductor loss is caused by the finite conductivity of strip conductor and ground plane conductor. The conductor loss is usually a predominant factor causing attenuation in the propagating EM wave. The current density near to the edge of a conductor is high that gives higher conductor loss. The conductor loss depends on the skin-depth and the surface resistivity of a conductor. Both these factors are present for a finite or infinite extent microstrip line. The conductor loss is computed by Wheeler's incremental rule and also by the perturbation method. Normally, Wheeler's model is applicable to a thickness strip conductor for $t \geq 7\delta_{\text{s}}$. However, with different formulations it could be applied even for the case, $t \geq 1.1\delta_{\text{s}}$. On comparing the results of conductor loss against the results of EM simulator, we have noted that Wheeler's model is satisfactory for $t \geq 2\delta_{\text{s}}$. The operating range for computation of conductor loss of a microstrip is divided in three parts-low-frequency range, medium-frequency range and high-frequency range. Wheeler's model is not applicable to the low- and medium-frequency ranges, whereas perturbation method is applicable to medium- and high-frequency ranges. The low-frequency range, $f \leq f_{\text{T1}}$ is determined by the following expression:

$$f_{\text{T1}} = \frac{R}{2\pi L} \tag{19}$$

where f_{T1} is the first critical frequency below which current is uniformly distributed inside the conductor giving DC conductor loss. R is the resistance p.u.l. of microstrip line given by

$$R = \frac{1}{\sigma(0) w t} \tag{20}$$

L is microstrip line inductance p.u.l. given by

$$L = \frac{Z_0(w_{\text{eff}},\ h,\ t,\ \varepsilon_{\text{r}} = 1, f = 0)}{c} \quad c = 3 \times 10^8\ \text{m/s} \tag{21}$$

Above the first transition frequency f_{T1}, the EM-field penetration appears causing strip effect phenomenon. The skin effect matures at another transition frequency given below which corresponds to $t = 2\delta_{\text{s}}$. Normally, Wheeler's incremental inductance rule is properly applicable above this frequency

$$f_{\text{T2}} = \frac{4}{\pi\mu\sigma_0 t^2} \tag{22}$$

where σ_0 is the static conductivity of the strip conductor. However, it has been noted that frequency-dependent conductivity provides better results on the conductor loss of a microstrip in mm-wave range. The empirically suggested expression is given below:

$$\sigma(f) = \sigma_0 \cdot \sqrt{1 + C_0 \cdot f_{\text{GHz}}} \quad C_0 = 0.045 \tag{23}$$

where frequency is in GHz and constant C_0 could be adjusted to improve the computed results. This aspect is discussed after comparison of both models against the results of EM simulator. However, empirical arrangement could provide acceptable results useful for microwave analogue circuit and over wide-frequency range the conductivity may also follow Debye's relaxation law:

$$\delta_{\text{s}} = \frac{1}{\sqrt{\pi f \mu \sigma(f)}} \tag{24}$$

The skin-depth δ_{s} inside a conductor is also modified accordingly.

(i) *DC loss:* The current inside the strip conductor is uniformly distributed for the frequency $f < f_{\text{T}}$. In that case, the conductor loss is computed from the following expression, which is used to compute the DC loss of a conductor:

$$\alpha_{\text{c}} = \frac{1}{2\sigma_0 w \cdot t \cdot Z_{\text{L}}(w_{\text{eff}},\ h,\ t,\ \varepsilon_{\text{r}}, f)} \text{Np/m} \tag{25}$$

where w is the strip width and t is its thickness. The strip thickness-dependent characteristic impedance of microstrip $Z_{\text{L}}(w_{\text{eff}},\ h,\ t,\ \varepsilon_{\text{r}}, f)$ is determined using (18).

(ii) *Wheeler's incremental inductance rule:* Wheeler's incremental inductance rule is a powerful tool for determination of conductor losses of TEM and quasi-TEM lines. The incremental inductance rule is derived from the surface impedance condition. The strength of inductance rule is in the fact that it avoids calculation of current density on the surface of the conductor. However, normally it is applicable to strip conductor for $t \geq 7\delta_{\text{s}}$ and with different formulations it could apply even for the case $t \geq 1.1\delta_{\text{s}}$. We summarise below expressions of Wheeler's model for microstrip line in terms of differential characteristic impedance caused by the field penetration. The magnetic field penetration inside the conductor causes change in the line inductance. Therefore, conductor loss is given by

$$\alpha_{\text{c}} = \frac{\omega \cdot \Delta L}{2 \cdot Z_0} = \frac{\omega \cdot \Delta Z_0}{2 \cdot V_{\text{p}} \cdot Z_0(w_{\text{eff}},\ h,\ \varepsilon_{\text{r}} = 1)} \quad \text{Np/m}$$

$$\alpha_{\text{c}} = \frac{\pi}{\lambda_0} \sqrt{\varepsilon_{\text{r eff}}(\Delta w,\ h,\ t,\ \varepsilon_{\text{r}}, f)} \times \frac{\Delta Z}{Z_0(w_{\text{eff}},\ h,\ \varepsilon_{\text{r}} = 1)} \quad \text{Np/m} \tag{26}$$

The strip conductor thickness-dependent characteristic impedance of a microstrip line on air substrate is determined using (17). The differential characteristic impedance is given by

$$\Delta Z = Z_0'(w'_{\text{eff}},\ h,\ \varepsilon_{\text{r}} = 1) - Z_0(w_{\text{eff}},\ h,\ \varepsilon_{\text{r}} = 1) \tag{27}$$

where effective width of microstrip line taking both conductor thickness and skin-depth penetration is given by

$$w'_{\text{eff}}(w,\ h,\ t,\ \delta_{\text{c}}) = w + \Delta w'_{\text{eff}}(a),$$

$$\Delta w'_{\text{eff}} = \begin{cases} \dfrac{(t - \delta_{\text{c}})}{\pi} \cdot \left(1 + \ln \dfrac{4 \cdot \pi \cdot (w - \delta_{\text{c}})}{(t - \delta_{\text{c}})}\right) & \text{for } \dfrac{w}{h} \leq \dfrac{1}{2\pi} \\ \dfrac{(t - \delta_{\text{c}})}{\pi} \cdot \left(1 + \ln \dfrac{2 \cdot (h - \delta_{\text{c}})}{(t - \delta_{\text{c}})}\right) & \text{for } \dfrac{w}{h} > \dfrac{1}{2\pi} \end{cases} \quad (b) \tag{28}$$

doi: 10.1049/joe.2017.0078

The modified characteristic impedance (MCI) of a microstrip with field penetration is obtained after modifying (17) suitably

$$Z'_0(w'_{\text{eff}},\ h,\ \varepsilon_r = 1) = \frac{377}{2\pi}\ln\left(F_1\frac{(h+\delta_s)}{w'_{\text{eff}}} + \sqrt{1+\left(\frac{2(h+\delta_s)}{w'_{\text{eff}}}\right)^2}\right) \quad (a)$$

$$F_1 = 6.0 + (2\pi - 6)\cdot\exp\left(-\left(30.666\cdot\frac{(h+\delta_s)}{w'_{\text{eff}}}\right)^{0.7528}\right) \quad (b) \tag{29}$$

(iii) *Perturbation's method:* The perturbation method is applicable to both thin and thick strip conductors. The method is applied separately to the strip conductor and the ground plane. In case of the strip conductor, concept of stopping distance (Δ) is used in order to avoid edge singularity. In case of the ground plane, closed-form current distribution on the ground plane of the microstrip is used. The conductor loss of a microstrip line is a summation of the conductor loss on the strip (α_{cs}) and conductor loss on the ground plane (α_{cg})

$$\alpha_c = \alpha_{cs} + \alpha_{cg} \tag{30}$$

The conductor losses (α_{cs}) and (α_{cg}) are given by the following expressions.

Loss on strip and ground plane are given by

(see (31))

where surface resistance is given by

$$R_s = \sqrt{\frac{\pi\mu_0 f_{\text{Hz}}}{\sigma(f)}} \tag{32}$$

The empirical expression for the reciprocal of normalised stopping distance Δ as a function of normalised strip conductor thickness is given below:

(see (33))

where normalised parameters are given below.

Reciprocal normalised stopping distance: $y = t/\Delta$ (a)

$$\text{normalised strip thickness:} x = \frac{t}{2\cdot\delta_s} \quad (b) \tag{34}$$

Results of the models are compared against the results of FEM-based EM simulator from 10 MHz to 10 THz.

4.3 Comparison of results of the proposed MCL against EM simulator

We have discussed above three models – DC model, Wheeler's method and perturbation method to compute conductor loss of a microstrip line over frequency range 0.01 GHz–10 THz. We also noted that conductivity of the strip conductor involved in both modes could be either static or frequency dependent as empirically suggested by Konno 1999. Thus, combined together we get four models:

(i) *Model# A:* Perturbation method with static conductivity $\sigma(f = 0)$, i.e. $\sigma(0)$, (ii) *Model# B:* Wheeler's model with static conductivity $\sigma(f = 0)$, i.e. $\sigma(0)$ **(iii)** *Model# C:* Perturbation method with frequency-dependent conductivity $\sigma(f)$, and (iv) *Model# D:* Wheeler's model with frequency-dependent conductivity $\sigma(f)$. We compare validity of above four models against the EM-simulated conductor loss of a microstrip line over frequency range 0.01 GHz–10 THz, *w/h* 0.1–10 and *t/h* 0.01–0.2. The aluminium conductor microstrip line taken on substrate with $\varepsilon_r = 11.9$, $h = 0.45$ mm is examined. The dielectric substrate is treated as lossless, i.e. tan $\delta = 0$. Figs. 4*a*–*c*–6*a*–*c* compare all four models including DC model against the results of EM simulator for $w/h = 0.1$, 1.0 and 10.0, respectively. Each width of microstrip line is examined for the conductor loss behaviour over frequency ranges 0.01 GHz–10 THz for $t/h = 0.01$, 0.05 and 0.2. For frequency below the first transition frequency, i.e. $f < f_{T1}$, the DC conductor loss is applicable in all cases. In between both transition regions model# A, i.e. the perturbation method with static conductivity could be better choice. The second transition f_{T2} is 0.05 GHz. The frequency range 1.0–100 GHz of the model# C provides average deviation about 2% for strip width $w/h = 0.1$, 1.0 and strip thickness $t/h = 0.01$, 0.05. For thick conductor $t/h = 0.2$ Wheeler's model# D could be used. However in some cases, we may use static conductivity model. Frequency range 100 GHz–1.0 THz, for $w/h = 0.1$, 1.0, the perturbation model# C is a better choice. However, for $w/h = 10.0$, Wheeler's model# D shows better agreement. In frequency range 1.0–10.0 THz, no model works satisfactorily. However, the models# A and # B with static conductivity could be used as a compromise.

5 Proposed integrated closed-form model analysis

We can form an *integrated closed-form model* from above-discussed individual models. The integrated model can compute frequency-dependent effective relative permittivity, characteristic

$$\alpha_{cs} = \frac{R_s}{4\cdot Z_L(w_{\text{eff}},\ h,\ t,\ \varepsilon_r,\ f)}\cdot\left(\frac{2}{2\pi w}\right)\cdot\ln\left(\frac{w-\Delta}{\Delta}\right) \quad (a)$$

$$\alpha_{cg} = \frac{R_s}{\pi\cdot w\cdot Z_L(w_{\text{eff}},\ h,\ t,\ \varepsilon_r,\ f)}\cdot\left\{\tan^{-1}\left(\frac{w}{2h}\right) - \frac{h}{w}\cdot\ln\left[1+\left(\frac{w}{2h}\right)^2\right]\right\} \quad (b) \tag{31}$$

$$y = \begin{cases} -60.89\cdot x^4 + 282.17\cdot x^3 - 27.764\cdot x^2 + 0.5103\cdot x + 9.1907 & \text{for } 0.03 \le x < 0.64 \\ 711.01\cdot x^6 - 2120.2\cdot x^5 - 1038.3\cdot x^4 + 9881.7\cdot x^3 - & \\ 12798\cdot x^2 + 6935.8\cdot x - 1372.7 & \text{for } 0.64 \le x < 1.5 \\ -183.05\cdot x^4 + 1583\cdot x^3 - 4981.9\cdot x^2 + 6618.6\cdot x - 2807.6 & \text{for } 1.5 \le x < 2.76 \\ 0.2953\cdot x^4 - 7.7733\cdot x^3 + 73.991\cdot x^2 - 293.88\cdot x + 581.98 & \text{for } 2.76 \le x < 8.0 \\ -0.0198\cdot x^3 + 0.9848\cdot x^2 - 12.104\cdot x + 240.01 & \text{for } 8.0 \le x < 16 \end{cases} \tag{33}$$

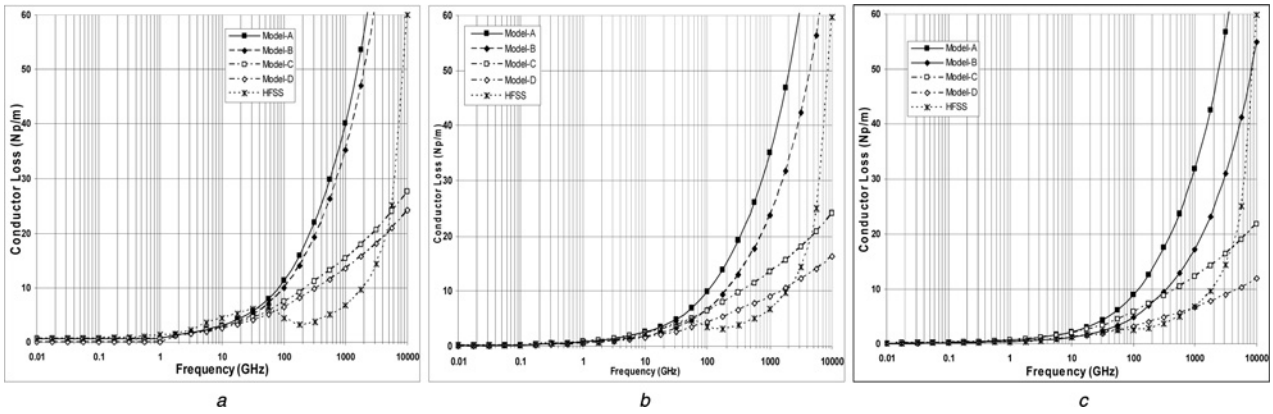

Fig. 4 *Conductor loss for w/h = 0.1, h = 0.45 mm, $\varepsilon_r = 11.9$*
a t/h = 0.01
b t/h = 0.05
c t/h = 0.2

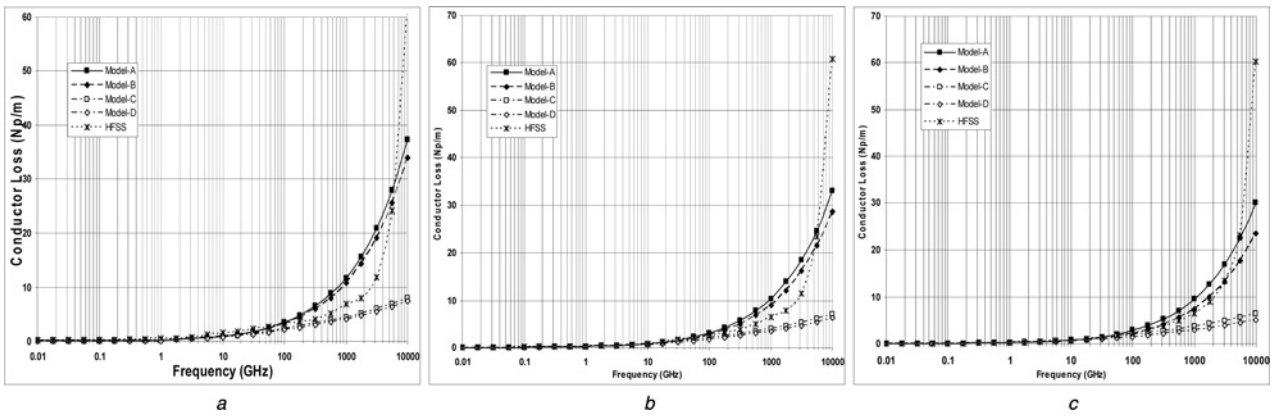

Fig. 5 *Conductor Loss for w/h = 1.0, h = 0.45 mm, $\varepsilon_r = 11.9$*
a t/h = 0.01
b t/h = 0.05
c t/h = 0.2

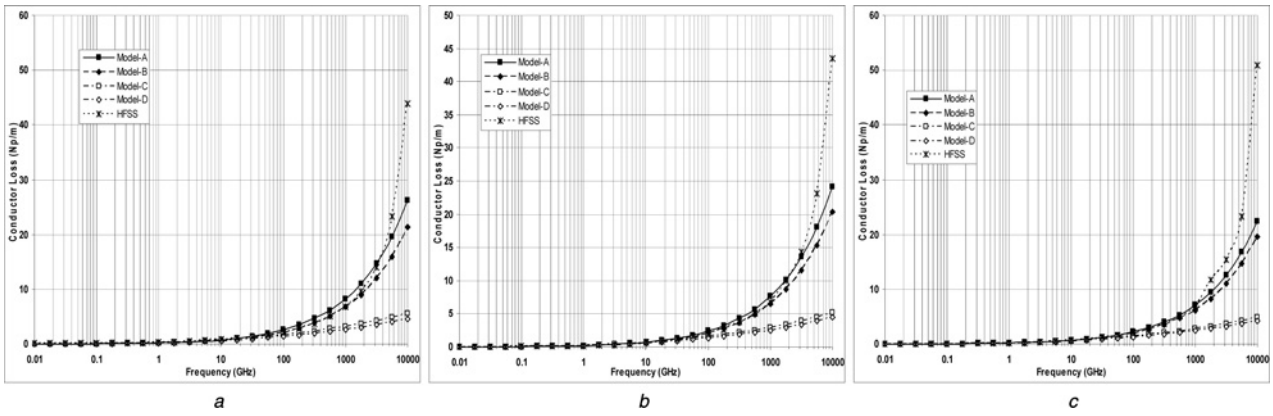

Fig. 6 *Conductor loss for w/h = 10.0, h = 0.45 mm, $\varepsilon_r = 11.9$*
a t/h = 0.01
b t/h = 0.05
c t/h = 0.2

impedance, dielectric loss and conductor loss from 0.01 GHz–10 THz for loss microstrip with relative permittivity $1 < \varepsilon_r < 200$. The conductor thickness is $t \leq 0.2$ and strip width is $0.1 \leq w/h \leq 10$. Accuracy of the integrated model is same as the accuracy of its individual component in various parametric ranges. To develop an integrated programme the following guide line is kept in mind:

(a) *Effective relative permittivity:* The MKJ-dispersion model is used for $\varepsilon_r \leq 200$.

doi: 10.1049/joe.2017.0078

(b) *Dielectric loss:* The validity of the dielectric models is suggested in (16). The dielectric loss models# 2 and # 4 find application in the integrated model.
(c) *Conductor loss:* It is more complicated consideration. Our primary models are DC model, Wheeler's method and perturbation method.

Below first transition frequency we should use DC model. Between two transition frequencies f_{T1} and f_{T2}, we should use static perturbation model# A. It is useful up to 1.0 GHz. For thin conductor $t/h < 0.05$, and narrow line $w/h \leq 1.0$ we should use perturbation model# C. However, for thick conductor and also wide strip conductor above these ranges for t/h and w/h, Wheeler's method is preferable.

On the basis of the observation, we are given a summary below for writing up the code for the integrated model. The grouping is done based on w/h. Next, it is subdivided based on t/h, which further subdivided based on the guided wavelength ($\lambda_g = \lambda_0/\sqrt{\varepsilon_r}$) range. The total scheme is summarised below:

Group# A: $w/h = 0.1$

(a) $t/h = 0.01$ – (i) $8.70\,\text{m} \leq \lambda_g \leq 0.087\,\text{m}$: DC model given in (25). It corresponds to 0.01–1.0 GHz for substrate $\varepsilon_r = 11.9$. (ii) $0.087\,\text{m} \leq \lambda_g \leq 0.87\,\text{mm}$: Model# A. It corresponds to 1.0–100 GHz. (iii) $0.87\,\text{mm} \leq \lambda_g \leq 0.0087\,\text{mm}$: Model# D. It corresponds to 100–10,000 GHz.
(b) $t/h = 0.05$ – (i) $8.7\,\text{m} \leq \lambda_g \leq 2.9\,\text{m}$: DC model. It corresponds to 0.01–0.03 GHz. (ii) $2.9\,\text{m} \leq \lambda_g \leq 0.087\,\text{m}$: Model# A. It corresponds to 0.03–1.0 GHz. (iii) $0.087\,\text{m} \leq \lambda_g \leq 0.87\,\text{mm}$: Model# B. It corresponds to 1.0–100 GHz. (iv) $0.87\,\text{mm} \leq \lambda_g \leq 0.0087\,\text{mm}$: Model# D. It corresponds to 100–10,000 GHz.
(c) $t/h = 0.2$ – (i) $8.7\,\text{m} \leq \lambda_g \leq 0.87\,\text{mm}$: Model# B. It corresponds to 0.01–100 GHz. (ii) $0.87\,\text{mm} \leq \lambda_g \leq 0.0087\,\text{mm}$: Model# D. It corresponds to 100–10,000 GHz.

Group# B: $w/h = 1$

(a) $t/h = 0.01$ – (i) $8.7\,\text{m} \leq \lambda_g \leq 0.17\,\text{m}$: DC model. It corresponds to 0.01–0.5 GHz. (ii) $0.17\,\text{m} \leq \lambda_g \leq 0.87\,\text{m}$: Model# A. It corresponds to 0.5–100 GHz. (iii) $0.87\,\text{mm} \leq \lambda_g \leq 0.0087\,\text{m}$: Model# C. It corresponds to 100–10,000 GHz.
(b) $t/h = 0.05$ – (i) $8.7\,\text{m} \leq \lambda_g \leq 2.9\,\text{m}$: DC model. It corresponds to 0.01–0.03 GHz. (ii) $2.9\,\text{m} \leq \lambda_g \leq 0.87\,\text{mm}$: Model# A. It corresponds to 0.03–100 GHz. (iii) $0.87\,\text{mm} \leq \lambda_g \leq 0.0087\,\text{mm}$: Model# C. It corresponds to 100–10,000 GHz.
(c) $t/h = 0.2$ – (i) $8.7\,\text{m} \leq \lambda_g \leq 0.87\,\text{m}$: Model# A. It corresponds to 0.01–0.1 GHz. (ii) $0.87\,\text{m} \leq \lambda_g \leq 0.0087\,\text{mm}$: Model# D. It corresponds to 0.1–10,000 GHz.

Group# C: $w/h = 10$

(a) $t/h = 0.01$ – (i) $8.7\,\text{m} \leq \lambda_g \leq 0.87\,\text{m}$: DC model. It corresponds to 0.01–0.1 GHz. (ii) $8.7\,\text{m} \leq \lambda_g \leq 8.7\,\text{m}$: Model# A. It corresponds to 0.1–10 GHz. (iii) $8.7\,\text{mm} \leq \lambda_g \leq 0.0087\,\text{m}$: Model# B. It corresponds to 10–10,000 GHz.
(b) $t/h = 0.05$ – (i) $8.7\,\text{m} \leq \lambda_g \leq 0.087\,\text{m}$: Model# A. It corresponds to 0.1–1.0 GHz. (ii) $0.087\,\text{m} \leq \lambda_g \leq 0.087\,\text{mm}$: Model# B. It corresponds to 1.0–1000 GHz. (iii) $0.087\,\text{m} \leq \lambda_g \leq 0.0087\,\text{mm}$: Model# C. It corresponds to 1000–10,000 GHz.
(c) $t/h = 0.2$ – (i) $8.7\,\text{m} \leq \lambda_g \leq 0.0087\,\text{mm}$: Model# B. It corresponds to 0.01–10,000 GHz.

6 Circuit model analysis

We have designed an integrated model for a practical microstrip line that computes separately dispersion, i.e. frequency dependent, effective relative permittivity and characteristic impedance. However, for a lossy microstrip line both these parameters are complex. Therefore, the integrated model is not a realistic model. Similarly, it computes separately the dielectric and conductor losses, whereas to some extent influenced by the propagation parameters. This aspect could account for by the circuit model of a microstrip line as shown in Fig. 7. Therefore, to extract resistance inductance capacitance conductance (RLCG) line parameters from the integrated model is required. The accuracy of the model could also be tested against the results from full-wave EM simulator.

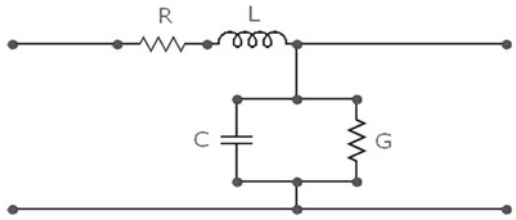

Fig. 7 *Equivalent circuit model of microstrip transmission line*

6.1 RLCG parameters

The primary line parameters RLCG p.u.l. is obtained from the results of dispersion $\varepsilon_{r\,\text{eff}}(w_{\text{eff}},\ h,\ t,\ \varepsilon_r,\ f)$, characteristic impedance $Z_0(w_{\text{eff}},\ h,\ t,\ \varepsilon_r,\ f)$, and dielectric loss $\alpha_d(w_{\text{eff}},\ h,\ \tan\delta,\ \varepsilon_r,\ f)$ and conductor loss $\alpha_c(w_{\text{eff}},\ h,\ t,\ \tan\delta = 0,\ \varepsilon_r,\ f)$. These are obtained under low-loss condition from the integrated model discussed previously. These expressions are summarised below:

$$
\begin{aligned}
R &= 2 \cdot Z_0(w_{\text{eff}},\ h,\ t,\ \varepsilon_r,\ f) \cdot \alpha_c && (a)\\
L &= Z_L(w_{\text{eff}},\ h,\ t,\ \varepsilon_r,\ f)\sqrt{\varepsilon_{r\,\text{eff}}(w_{\text{eff}},\ h,\ t,\ \varepsilon_r,\ f)}/c_0 && (b)\\
C &= \sqrt{\varepsilon_{r\,\text{eff}}(w_{\text{eff}},\ h,\ t,\ \varepsilon_r,\ f)}/c_0 \cdot Z_0(w_{\text{eff}},\ h,\ t,\ \varepsilon_r,\ f) && (c)\\
G &= 2\alpha_d/Z_0(w_{\text{eff}},\ h,\ t,\ \varepsilon_r,\ f) && (d)
\end{aligned}
\tag{35}
$$

The RLCG could be used to compute propagation parameters of a practical line correctly that is useful for analogue circuit design using microstrip up to THz range.

6.2 Transmission line parameters from circuit model

The complex characteristic impedance and complex propagation constant are obtained from frequency and conductor thickness-dependent RLCG parameters as follows:

$$
\begin{aligned}
Z_0^*(f,\ t) &= \sqrt{\frac{R(f,\ t) + \mathrm{j}\omega L(f,\ t)}{G(f) + \mathrm{j}\omega C(f,\ t)}} && (a)\\
\gamma*(f,\ t) &= \alpha_T(f,\ t) + \mathrm{j}\beta(f,\ t)\\
&= \sqrt{\big(R(f,\ t) + \mathrm{j}\omega L(f,\ t)\big)\big(G(f,\ t) + \mathrm{j}\omega C(f,\ t)\big)} && (b)\\
\varepsilon_{r\,\text{eff}}(f,\ \alpha) &= (\beta/\beta_0)^2 && (c)
\end{aligned}
\tag{36}
$$

where total loss of a microstrip line is $\alpha = \alpha_c + \alpha_d$.

In the next section, we compare the results of circuit model against the results of full-wave EM simulator. We also present curve-fitted models of dispersion and total loss of a lossy microstrip line based on the data obtained from full-wave EM simulator.

6.3 HFSS-based models

The data on effective relative permittivity and the total loss of three microstrip line, $w/h = 0.1,\ 1.0,\ 10$ on substrate with $\varepsilon_r = 11.9$, $h = 0.45$ mm, $\tan\delta = 0.001$ and strip thickness $t/h = 0.05$ with strip

doi: 10.1049/joe.2017.0078

conductivity $\sigma_0 = 3.8 \times 10^7$ S/m are generated using full-wave EM simulator. The polynomial curve fitting is carried out for the effective relative permittivity in three frequency ranges, whereas for the total losses are also calculated in four frequency ranges. The results are presented in (37)–(42) for $w/h = 0.1$, 1.0 and 10, respectively.

(i) (i) Microstrip line # 1: $w/h = 0.1$

(see (37))

(see (38))

(ii) (ii) Microstrip line # 2: $w/h = 1.0$

(see (39))

(see (40))

(iii) (iii) Microstrip line # 2: $w/h = 10$

(see equation (41) at the bottom of the next page)

(see equation (42) at the bottom of the next page)

Figs. 8–10 compare the circuit model and the curve-fitted dispersion and total loss models against the results from full-wave EM simulator for $w/h = 0.1$, 1.0 and 10. In case of $w/h = 0.1$, the curve-fitted full-wave EM simulator (HFSS) model has maximum deviation 1.5% and average deviation 0.8% for the effective relative permittivity. The circuit model has maximum deviation 4.0% and average deviation 2.5%. It is obvious from Fig. 8*a* that more deviation occurs in the slow-wave region below 1.0 GHz. The slow wave is due to the finite conductivity of strip and ground

$$\varepsilon_{\text{reff}}(f) = \begin{cases} 62.639(f)^6 - 214.97(f)^5 + 288.96(f)^4 - 192.69(f)^3 + 66.845(f)^2 \\ -11.803(f) + 7.4058, & (0.01 \le f \le 1.0) \\ 710^{-06}(f)^6 - 0.0003(f)^5 + 0.004(f)^4 - 0.0304(f)^3 + 0.1281(f)^2 \\ -0.2779(f) + 6.5577, & (1.0 \le f \le 10) \\ -7.0 \times 10^{-17}(f)^6 + 3.0 \times 10^{-13}(f)^5 - 5.0 \times 10^{-10}(f)^4 + 5.0 \times 10^{-0}7(f)^3 \\ -0.0002(f)^2 + 0.0601(f) + 5.387 & (10.0 \le f \le 1000) \end{cases} \tag{37}$$

$$\text{loss(Np/m)} = \begin{cases} -0.0001 \times (f)^6 + 0.0032 \times f)^5 - 0.0388 \times (f)^4 + 0.227 \times (f)^3 \\ -0.6472 \times (f)^2 + 0.9767 \times (f) + 0.1921, & (0.01 \le f \le 10) \\ 3.0 \times 10^{-09}(f)^6 - 5.0 \times 10^{-07}(f)^5 - 4.0 \times 10^{-05}(f)^4 - 0.0016(f)^3 \\ +0.0327(\text{f})^2 - 0.1762(f) + 2.1493 & (10 \le f \le 50) \\ -9.0 \times 10^{-13}(f)^6 + 9.0 \times 10^{-10}(f)^5 - 4.0 \times 10^{-07}(f)^4 + 8.0 \times 10^{-05}(f)^3 \\ -0.0086(f)^2 + 0.48(f) - 4.1732 & (50 \le f \le 250) \\ -3.0 \times 10^{-18}(f)^6 + 1.0 \times 10^{-14}(f)^5 - 3.0 \times 10^{-11}(f)^4 + 4.0 \times 10^{-08}(f)^3 \\ -3.0 \times 10^{-05}(f)^2 + 0.0162(f) + 4.0646 & (50 \le f \le 1000) \end{cases} \tag{38}$$

$$\varepsilon_{\text{reff}}(f) = \begin{cases} 25.915(f)^6 - 90.266(f)^5 + 123.76(f)^4 - 84.78(f)^3 + 30.52(f)^2 \\ -5.6474(f) + 7.5879 & (0.01 \le f \le 1.0) \\ 3.0 \times 10^{-06}(f)^6 - 0.0001(f)^5 + 0.0016(f)^4 - 0.0123(f)^3 \\ +0.0537(f)^2 - 0.1124(f) + 7.1533 & (1.0 \le f \le 10) \\ -3.0{*}10^{-16}(f)^6 + 1.0 \times 10^{-12}(f)^5 - 1.0 \times 10^{-09}(f)^4 + 1.0 \times 10^{-06}(f)^3 \\ -0.0004(f)^2 + 0.0654(f) + 6.9318 & (10 \le f \le 1000) \end{cases} \tag{39}$$

$$\text{loss(Np/m)} = \begin{cases} -04.0 \times 10^{-05}(f)^6 + 0.0013(f)^5 - 0.0154(f)^4 + 0.0898(f)^3 \\ -0.2495(f)^2 + 0.3784(f) + 0.078 & (0.01 \le f \le 10) \\ -2.0 \times 10^{-16}(f)^6 + 8.0 \times 10^{-13}(f)^5 - 1.0 \times 10^{-09}(f)^4 \\ +8.0 \times 10^{-07}(f)^3 - 0.0003 \times (f)^2 + 0.0626 \times (f) + 0.848 & (10 \le f \le 1000) \end{cases} \tag{40}$$

doi: 10.1049/joe.2017.0078

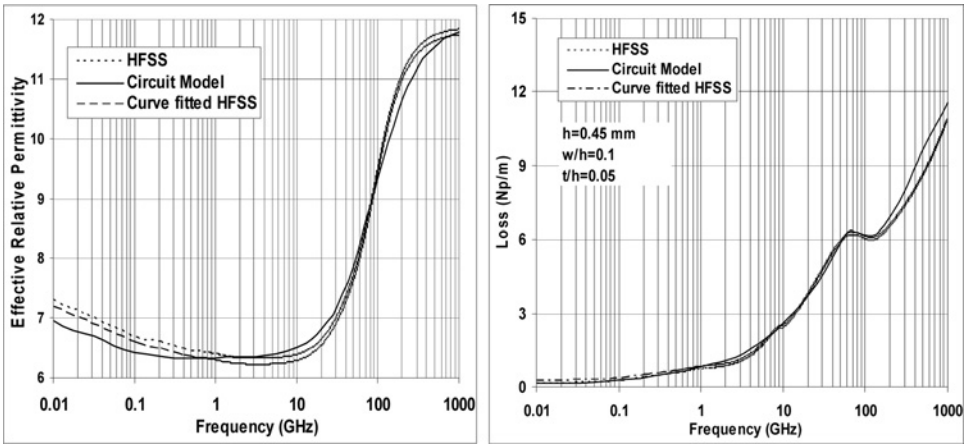

Fig. 8 *Comparison of effective relative permittivity and total loss w/h = 0.1, h = 0.45 mm, t/h = 0.05*

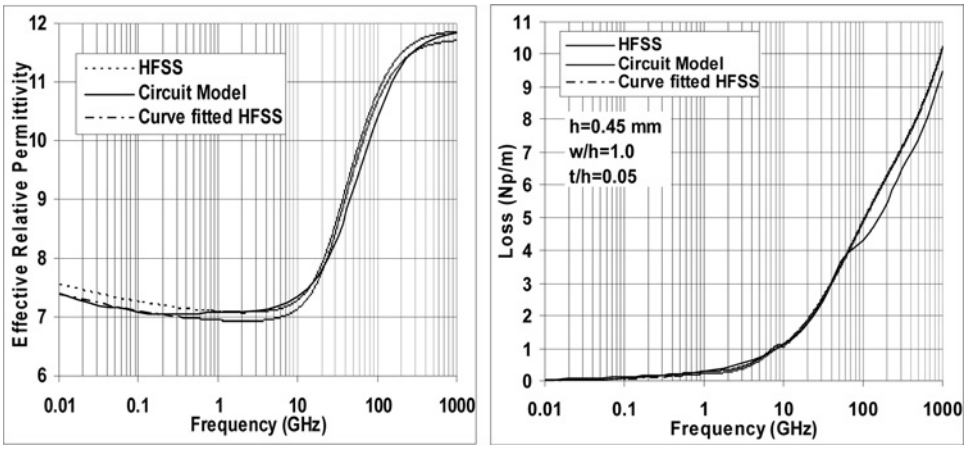

Fig. 9 *Comparison of effective relative permittivity and total loss w/h = 1.0, h = 0.45 mm, t/h = 0.05*

conductors. In case of $w/h = 0.1$, the curve-fitted full-wave EM simulator model has average deviation 5.0% for the total loss. The circuit model has average deviation 8.0%. We note from Fig. 8*b* that deviation in circuit model for total loss increases only above 200 GHz.

In case of $w/h = 1.0$, the deviations for dispersion between the curve-fitted model against full-wave EM simulator data has reduced to maximum deviation 2.5% and average deviation 1.45%. Similarly, for the circuit model it has reduced to maximum deviation 2.7% and average deviation 2.2%. For total loss modelling, improvement in the circuit models is minor. The average deviation for the curve-fitted model is 5.0%, whereas for the circuit model it is 7.0%. Figs. 9*a* and *b* support these observations.

$$\varepsilon_{reff}(f) = \begin{cases} 23.164(f)^6 - 79.359(f)^5 + 107.01(f)^4 - 72.117(\mathrm{f})^3 \\ +25.633(f)^2 - 4.707(f) + 10.048 \qquad (0.01 \le f \le 1.0) \\ 3.0 \times 10^{-06}(f)^6 - 0.0001(f)^5 + 0.0025(f)^4 - 0.0259(f)^3 \\ +0.13(f)^2 - 0.1301(f) + 9.6904 \qquad (1.0 \le f \le 10) \\ -3.0 \times 10^{-16}(f)^6 + 1.0 \times 10^{-12}(f)^5 - 1.0 \times 10^{-09}(f)^4 \\ +1.0 \times 10^{-06}(f)^3 - 0.0004(f)^2 + 0.0654(f) + 6.9318 \quad (10.0 \le f \le 1000) \end{cases} \tag{41}$$

$$\mathrm{loss(Np/m)} = \begin{cases} -6.0 \times 10^{-06}(f)^6 + 0.0002(f)^5 - 0.0029(f)^4 + 0.0186(f)^3 \\ -0.0622(f)^2 + 0.2073(f) + 0.0852 \qquad (0.01 \le f \le 10) \\ -2.0 \times 10^{-16}(f)^6 + 5.0 \times 10^{-13}(f)^5 - 8.0 \times 10^{-10}(f)^4 + 6.0 \times 10^{-07}(f)^3 \\ -0.0002(f)^2 + 0.0561(f) + 0.726 \qquad (10 \le f \le 1000) \end{cases} \tag{42}$$

doi: 10.1049/joe.2017.0078

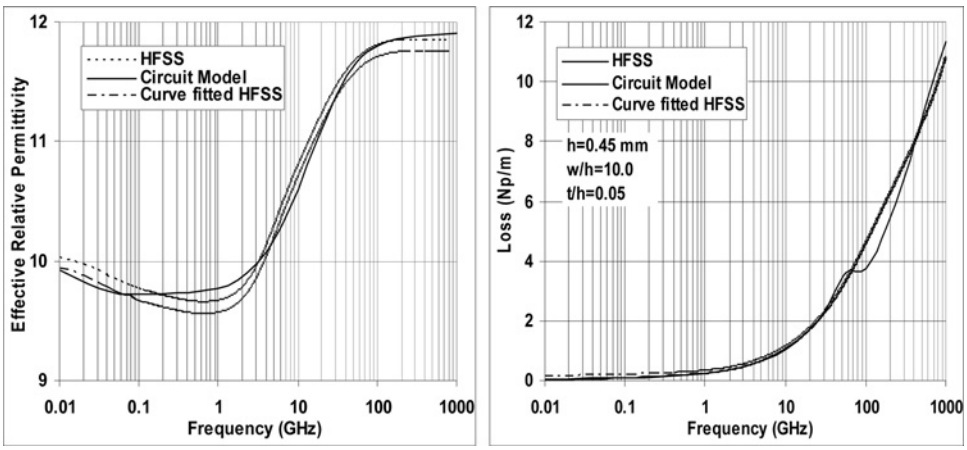

Fig. 10 *Comparison of effective relative permittivity and total loss w/h = 10.0, h = 0.45 mm, t/h = 0.05*

In case of $w/h = 10.0$, the deviations for dispersion computed by the curve-fitted model are 3.2% for maximum deviation and 1.36% for average deviation. For the circuit model, these maximum and average deviations are 3.7 and 2.3%, respectively. Similarly, for the total loss the curve-fitted model has average deviation 4.5%, whereas the circuit model has average deviation 5.0% as shown in Figs. 10*a* and *b*.

In conclusion, we can say that the circuit model results have same order of deviation from the results of full-wave EM simulator, as it occurs between full-wave methods and various EM simulators. The validity of the circuit model is further examined for more lossy substrate and lossy strip conductors; as these lines are important for THz interconnects technology.

6.4 Further validation of circuit models

In the above section, we checked accuracy of the microstrip of aluminium conductors on standard low-lossy substrate $\varepsilon_r = 11.9$, $h = 0.45$ mm, $t/h = 0.05$, $\tan\delta(0) = 0.001$ for $w/h = 0.1$, 1.0, 10.0 with average deviation 2.5–3.3% for the dispersion and 3.4–4.7% for the total loss. However, in very large scale integration (VLSI) technology [29] we use aluminium ($\sigma_0 = 3.7 \times 10^7$ S/m), tungsten ($\sigma_0 = 1.0 \times 10^7$ S/m) and tungsten–silicide ($\sigma_0 = 3.3 \times 10^6$ S/m) conductors**.** The microstrip with these conductors are fabricated on the Si substrate with $\varepsilon_r = 11.9$ and $h = 450$ μm [30–34]**.** We noted that lower conductivity for last two conductors and its results in high conductor loss and stronger slow-wave factor in low-frequency range. In this section, validity of the integrated and circuit models against the results of full-wave EM simulator over frequency range 0.01 GHz—1.0 THz.

We considered microstrip line of three conductors mentioned above on the Si substrate with $\varepsilon_r = 11.9$, $h = 450$ μm. The strip conductor thickness is $t = 0.5$ μm and $w/h = 0.67$ for all cases. The MKJ model is used in the integrated (direct) model and the perturbation method with $\sigma(f)$ used to compute the conductor loss by using MCL model. Fig. 11 compares both the dispersion and total loss as computed by the direct model and circuit model against the results of full-wave EM simulator for aluminium conductor with substrate resistivity of $\rho_s = 10\ \Omega$ cm and $\rho_s = 100\ \Omega$ cm. Similarly, tungsten and tungsten–silicide conductors were also studied for the above-mentioned substrate resistivity. The effective relative permittivity as shown in Fig. 11 is increased gradually below 10.0 GHz with decrease in frequency. This is known as slow-wave effect. It is due to the interaction of the conductor loss with the propagation constant. The circuit model follows the results of full-wave EM simulator faithfully. However, deviation increases with decrease in the conductivity of the strip conductor from aluminium to tungsten to tungsten–silicide. The direct model is not able to account the slow-wave effect in frequency range below 10 GHz.

We also note from Fig. 12 that the propagation constant is not having any significant effect on the total loss. Thus, results on total loss obtained from the circuit model and the direct model are almost same. However, deviation results for the loss increases with decrease in conductivity of both the strip conductor and Si

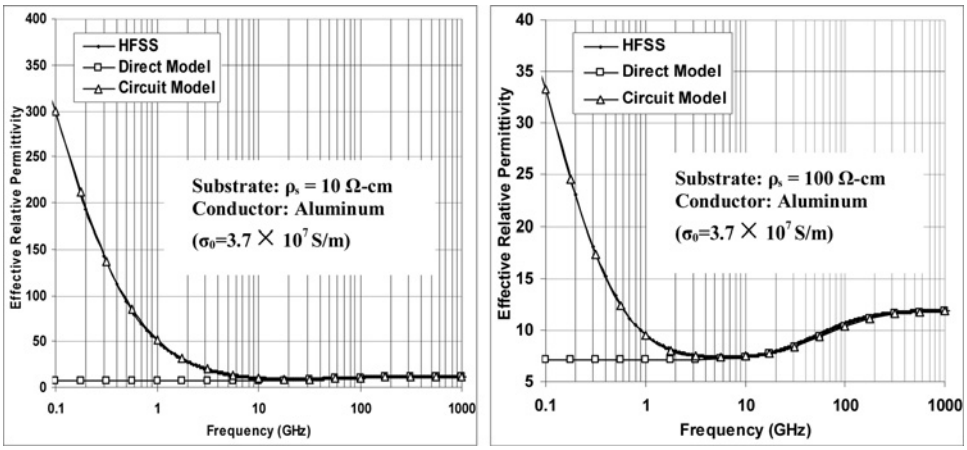

Fig. 11 *Comparisons of effective relative permittivity on substrates-*
a $\rho_s = 10\ \Omega$ cm
b $\rho_s = 100\ \Omega$ cm aluminium conductor

doi: 10.1049/joe.2017.0078

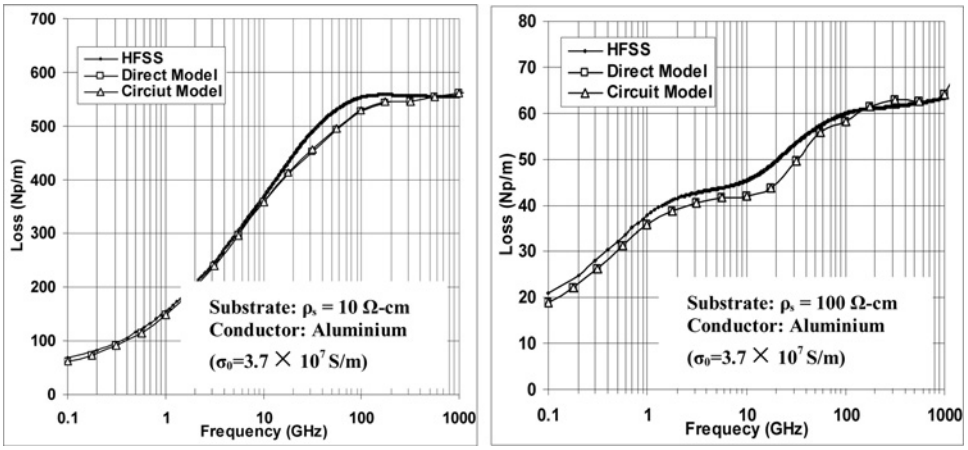

Fig. 12 *Comparisons of total loss (Np/m) on substrates-*
a $\rho_s = 10\ \Omega$ cm
b $\rho_s = 100\ \Omega$ cm aluminium conductor

substrate. For resistivity of substrate $\rho_s = 100\ \Omega$ cm, we note appearance of loss minimum, whereas there is no such minimum loss noted for $\rho_s = 10\ \Omega$ cm substrate. It appears that minimum loss valley appears for $\rho_s = 100\ \Omega$ cm substrate, as in this case conductor is more than the dielectric loss. We note that for tungsten–silicide conductor, minimum loss valley is more prominent as compared with that of aluminium and tungsten strip conductors on $\rho_s = 100\ \Omega$ cm substrate. Thus the circuit model, and also the components of integrated model, needs improvement in some cases, though it is within variation range in the loss computation by different simulators for several ranges.

7 Conclusion

This paper has presented a computer-aided design-based circuit model which will be applicable to microstrip transmission line as THz interconnects in circuit simulator. Comparison of MKJ model and characteristic impedance with full-wave EM simulator, which shows $< 1\%$ deviation for w/h range $0.1 \leq w/h \leq 100$, conductor thickness $0.001 \leq t/h \leq 0.2$, wavelength range $8.7\ \mu\text{m} \leq \lambda_g \leq 8.7$ m and substrate permittivity $1.0 \leq \varepsilon_r \leq 200$ was investigated. The formulations of MDL and MCL models were also compared with full-wave EM simulator which showed deviation of < 1 dB and calculation of RLCG(f) by using the effect of dispersion, characteristic impedance and losses which shows $< 1\%$ deviation with experimental data available. Accuracy of the circuit model also verified for interconnects made by aluminium ($\sigma_0 = 3.7 \times 10^7$ S/m), tungsten ($\sigma_0 = 1.0 \times 10^7$ S/m) and tungsten–silicide ($\sigma_0 = 3.3 \times 10^6$ S/m) conductors which are used in very large scale integration/ultra large scale integration (VLSI/ULSI) technology.

8 References

[1] Gu Q.J.: 'THz interconnect the last centimeter communication', *IEEE Commun. Mag.*, 2015, **53**, (4), pp. 206–215
[2] Yu B., Liu Y., Hu X.: 'Micromachined sub-THz interconnect channels for planar silicon processes'. IEEE Int. Microwave Symp., 2014
[3] Awasthi Y.K., Bansal R., Singh P.: 'Accurate dispersion model for microstrip line up to terahertz frequency range'. SPIE Int. Conf. Communication and Electronics System Design, 2013
[4] Schnieder F., Heinrich W.: 'Thin-film microstrip lines and coplanar waveguides on semiconductor substrates for sub-mm-wave frequencies', *Frequenz*, 2005, **59**, pp. 1–5
[5] Deutsch A.: 'On-chip wiring design challenges for GHz operation', *IEEE Proc.*, 2001, **89**, (4), pp. 529–554
[6] Kiziloglu K., Dagli N., Matthaei G.L.: 'Experimental analysis of transmission line parameters in high-speed GaAs digital circuit interconnects', *IEEE Trans. Microw. Theory Tech.*, 1991, **39**, (8), pp. 1361–1367
[7] Rivaz de S., Lacrevaz T., Gallitre M.: 'Dielectric loss effects on the modeling of interconnect responses for the 45 nm node', *IEEE Signal Propag. Interconnects*, 2008, **1–4**, pp. 12–15
[8] Eo Y., Eisenstadt W.R., Shim J.: 'S-parameter-measurement-based high-speed signal transient characterization of VLSI interconnects on SiO_2–Si substrate', *IEEE Adv. Packag.*, 2000, **23**, (3), pp. 470–479
[9] NASA Report, techport. nasa. gov: 'Robust micro-fabricated interconnect technologies: DC to THz project, 2015–2016'
[10] Haikun Z., Shi R., Chen H., *ET AL.*: 'Distortion minimization for packaging level interconnects'. IEEE Electrical Performance of Electronic Packaging, Scottsdale, AZ, USA, October 2006, pp. 175–178
[11] Awasthi Y.K., Singh H., Kumar A.: 'Accurate CAD-model analysis of multilayer microstrip line on anisotropic substrate', *J. Infrared Millim. Terahertz Waves*, 2010, **31**, (3), pp. 259–270
[12] Swanson D.G., Hoefer W.J.R.: 'Microwave circuit modeling using electromagnetic field simulation' (Artech House, Boston, 2003)
[13] Kirschning M., Jansen R.H.: 'Accurate wide-range design equations for the frequency-dependent characteristics of parallel coupled microstrip lines', *IEEE Trans. Microw. Theory Tech.*, 1985, **33**, p. 288
[14] Singh H., Verma A.K.: 'Closed-form model of shunt capacitance of microstrip step discontinuity'. IEEE Asia Pacific Microwave Conf., China, 2005, vol. **3**, pp. 4–7
[15] Brun C.: 'Carbon nanostructures dedicated to millimeter-wave to THz interconnects', *IEEE Trans. Terahertz Sci. Tech.*, 2015, **5**, (3), pp. 383–390
[16] Cam N.: 'Analysis methods for RF, microwave, and millimeter–wave planar transmission lines' (John Wiley & Sons, N.Y., 2000)
[17] Sadiku M.N.O., Musa S.M., Nelatury S.R.: 'Comparison of dispersion formulas for microstrip lines'. IEEE Southeast Conf. Proc., 2004, pp. 378–382
[18] Zhou Z., Melde K.L.: 'A comprehensive technique to determine the broad band physically consistent material characteristics of microstrip lines', *IEEE Trans. Microw. Theory Tech.*, 2010, **58**, (1), pp. 185–194
[19] Verma A.K., Kumar R.: 'A new dispersion model for microstrip line', *IEEE Trans. Microw. Theory Tech.*, 1998, **46**, (8), pp. 1183–1187
[20] Pengpeng S., Yin X., Hong W.: 'On dispersion in different position of microstrip line'. IEEE Asia-Pacific Microwave Conf., 2006, 1968–1971, pp. 12–15
[21] Heinrich W.: 'Conductor loss on transmission lines in monolithic microwave and millimeter-wave integrated circuits', *Int. J. Microw. Mm-wave Comput.-Aided Eng.*, 2007, **2**, (3), pp. 155–167
[22] Yamashita E., Atsuki K., Veda T.: 'An accurate dispersion formula of microstrip lines for computer added design of microwave integrated circuit', *IEEE Trans. Microw. Theory Tech.*, 1979, **27**, (12), pp. 1036–1038
[23] Krischning M., Jansen R.H., Koster N.H.L.: 'New aspects concerning the definition of microstrip characteristic impedance as a function of frequency'. IEEE MTT-S, Int. Microw. Symp. Dig., 1982, pp. 305–307

[24] Warwick C: 'Understanding the Kramers–Kronig relation using a pictorial proof' (Agilent EEsof EDA, USA., 2010), vol. **31**
[25] Chahal P.: 'Millimeter wave and terahertz dielectric probe microfluidic sensors'. IEEE 39th Int. Conf. Infrared, Millimeter, and Terahertz Waves, 2014, vol. **1-2**, pp. 14–19
[26] Zheng J., Hahm Y.C., Tripathi V.K.: 'CAD-oriented equivalent-circuit modeling of on-chip interconnects on lossy silicon substrate', *IEEE Trans. Microw. Theory Tech.*, 2000, **48**, (9), pp. 1443–1451
[27] Rautio J.C., Le Roy M.R., Rautio B.J.: 'Synthesis of perfectly causal parameterized compact models for planar transmission lines', *IEEE Trans. Microw. Theory Tech.*, 2009, **57**, (12), pp. 2938–2947
[28] Wu H.W., Weng M.H.: 'Effects of DC-bias conditions on low-loss thin film microstrip line'. Progress in Electromagnetics Research Conf., 2010, vol. **13**, pp. 19–32
[29] Willliams D.F.: 'Causal characteristics impedance of planar transmission lines', *IEEE Adv. Packag.*, 2003, **26**, (2), pp. 165–171
[30] Zhang J., Drewniak J.L., Pommerenke D.J.: 'Causal RLGC (f) models for transmission lines from measured S-parameters', *IEEE Electromagn. Compat.*, 2010, **52**, (1), pp. 189–198
[31] Goosen K.W., Hammond R.B.: 'Modeling of picosecond pulse propagation in microstrip interconnections on integrated circuits', *IEEE Trans. Microw. Theory Tech.*, 1989, **37**, (3), pp. 469–478
[32] Chen C.C.: 'High-performance bulk and thin-film microstrip transmission lines on VLSI-standard Si substrates', *Microw. Opt. Tech. Lett.*, 2004, **43**, (2), pp. 148–151
[33] Zhang L., Song J.M.: 'Transient signal distortion in silicon-based interconnects over thin-film metal ground layers'. IEEE Electrical Performance of Electronic Packaging, Scottsdale, AZ, USA, October 2006, pp. 145–148
[34] Gu Q.J.: 'Integrated circuits and systems for THz interconnect'. IEEE Wireless and Microwave Technology Conf., 2015, vol. **1–5**, pp. 13–15